Investigation of Structural, Optical And Electrochemical Properties of V_2O_5 Nanoparticles Prepared By Time Efficient Microwave Autoclave Technique

Rajesh V[1], Veeramuthu K[2], M Gunasekaran[3], Vignesh B[4]
[1, 2, 3, 4] Dept of Physics
[1, 2] Thiru Kolanjiappar Government Arts College, Vriddhachalam, Tamil Nadu, India - 606 001.
[3, 4] Muthurangam Government Arts College (A), Vellore, Tamil Nadu, India - 632 002.

Abstract- *The time-efficient microwave autoclave technique has been utilised to synthesise the V2O5 nanoparticles. According to XRD analysis, the progression of the nanostructure was in complete orthorhombic form, and using the Scherrer formula, the grain size (33.58 nm), dislocation density (δ), micro strain (ε), and all sub-oxide phases of the metal oxide were determined. The energy band gap (Eg) at the edge of the absorbance band was measured as 4.82 eV for a direct transition by using UV-Vis spectroscopic data and Tauc's relation. The complex dielectric constants (εr and εi) and refractive index (n) were computed by applying UV-Vis spectra. According to the FTIR vibrational spectrum, the various molecular vibrations and the V-O chemical bonding nature have been confirmed. An excellent PL spectrum was used to analyse the nanoparticles colour nature in the visible region. The morphological study has been done by applying a SEM analysis technique, and the appearance of nanoparticles with a dimension of V2O5 has been confirmed. The maximum specific capacity of the material was calculated using a CV analyzer and quantified using a GCD test to estimate the energy density and power density of the sample.*

Keywords- V_2O_5, Microwave autoclave, Specific capacitance, CV, GCD.

I. INTRODUCTION

In recent trends, the technological generation requires more energy-saving devices. They are essential for upcoming microelectronic devices, electric drives, automobiles, solid-state drives (SSD), LED flash lights, and communication systems. A supercapacitor plays a vital role in this regard. A decent number of researchers are currently exploring various types of supercapacitors, such as batteries with high power density and cyclic stability. The non-faradic and faradic processes determine the supercapacitor as an electric double-layer capacitor and a pseudo-capacitor, respectively. According to the electrostatic charge storage mechanism, the charging time and the discharge time are 100% consistent, provided the current is constant. As a result, the supercapacitor produces exorbitant cycles in a very short period of time. At room temperature, more than 1 million charge-discharge cycles can be achieved with less than 20% capacitance and 100% resistance[1]. Transition metal oxides obtain spin-half or free-d orbital electrons, which allow these types of electron valence to activate the absorption and desorption processes of different types of reactants[2-3]. According to the concept, the electrodes of the supercapacitors are formed by transition metal oxide materials. Electrodes designed specifically for supercapacitors significantly increase the capacitance and charge/discharge stability. The hydrous ruthenium oxide/activated carbon ($RuO_x.nH_2O$/AC) electrode possesses good electrochemical stability and a high specific capacitance of 1580 Fg^{-1}. Due to expense and contamination, this form of substance is often unavailable for use [4]. Vanadium oxide nanoparticles are used generally as smoke detectors, nitrogen gas sensors, solar windows, nanomedicine, automotives, and especially chromogenic effects, smart-soft contact lenses, self-robotics, and spintronic gadgets. In pseudocapacitors, these are highly recommended electrodes. In metal oxides, V_2O_5 has mixed oxidation states (V^{2+}, V^{3+}, V^{4+}, and V^{5+}), very low cost, nontoxicity, and is a high-specific capacitance electrode material[10]. In recent trends, researchers have mostly reported that very simple methods of sol-gel, hydrothermal, microwave irradiation, and thin film synthesis give very effective structure morphology, crystallisation, optical properties, and electrochemical performance in nano research. The microwave irradiation and autoclave methods are very simple, low-cost, low-toxic, and fast techniques for building nanoparticles with high precision measurement. The time-efficient microwave autoclave technique in which the nanoparticles are set has reached an enormous level of occurrence[5-6]. V_2O_5 molecules are heated up and precisely sorted as layered nanocrystalline when the material is

microwaved due to its electric dipole and layered structure. These layers are separated by a Van der Waal gap of 10–14 Å [5]. In storing the charges, ion intercalation and de-intercalation are involved. In this study, we elaborate on the synthesis of V_2O_5, its crystalline structure, surface morphology, optical properties, and electrochemical performance.

II. METHODOLOGY

The glassware was thoroughly cleaned in the laboratory with distilled water to prevent any contamination. The analytical grade chemicals only used. The key ingredient of this reaction is ammonium metavanadate (NH_4VO_3), which is highly soluble in water and produces no hazards during chemical reactions. Ammonium metavanadate was diluted to 1 mol in 50 ml of de-ionised (DI) water and stirred vigorously for 1 hr at ambient temperature until fully dissolved. Acetic acid (CH_3COOH) and polyvinyl alcohol (CH_2CHOH) were prepared as solutions in separate beakers, which were stirred continuously for a period of 1hr. Chemically, NH_4VO_3, acetic acid, and PVA were treated in a 1:1:1 ratio, with acetic acid acting as a reducing agent and PVA acting as a capping agent. The white NH_4VO_3 solution turns red when blended with acetic acid. The entire hue of the solution turns crimson after being heated at 80 ^oC for 2 hr, and it was obtained in the form of a broth. Without any chemical reaction, the stored solution was completely shifted to an autoclave. During the microwave combination process, the autoclave was irradiated for 6 hr at P-60 in a well-closed microwave oven (IFB-20SC3). The material extracted from the autoclave reaches room temperature in the oven, and that material was filtered several times after being washed with water and ethanol. The liquid molecules were then heated, and the precipitation obtained was dried on a hot plate. The dried material was heated in a muffle furnace at 550^oC for 3 hr. The end product was finely ground and extracted as powder particles, which were subjected to analysis to determine their characteristics.

III. MODELING AND ANALYSIS

Characterisation

Powder XRD (BRUKER-D8 advance at 30 kV and 10 mA with Cu Kα radiation λ = 1.5406) diffraction 2θ was recorded in the range of 0^o-90^o and the crystalline morphological composition and purity of the phases were assessed. Ultraviolet and visible (UV-Vis-Perkin Elmer, Lambda 35) absorption spectroscopy was used to investigate the optical properties. Photoluminescence spectroscopy (PL) was used to examine the various absorption wavelengths of a material. The frequency absorption of infrared radiation by a sample substance was measured using the Fourier transform infra-red spectrometer (FTIR). Molecular band vibrations were defined by infrared absorption bands. The scanning electron microscope (SEM) creates an image by scanning the surface with a targeted electron beam. The electrons in the beam interact with the sample, generating a variety of signals that were used to predict particle size and form. A three-electrode system electrochemical setup was used to conduct cyclic voltammetry (CV) and galvanostatic charge-discharge experiments (GCD).

Electrochemical studies

The electroanalytical approach of cyclic voltammetry is ideal for investigating the phase changes of redox couples during the Li^+ intercalation and deintercalation processes. The simple reaction used to induce electrochromism in the V=O system [7-8].

$$V_2O_5 + xLi^+ + xe^- \leftrightarrow Li_xV_2O_5$$

where 80% V_2O_5 is the active material, 15% activated carbon, and 5% PTFE (polytetrafluroethylene) is the binding agent to make the electrode. A few drops of ethanol were used as a solvent. 1 mg of the active substance was pasted onto an aluminium foil (1cm x 1cm and 1mm thickness) and allowed to dry at 70 ^oC for 1 hr. The gel electrolyte has been prepared by dissolving 0.5 M $NaSO_4$ in a 2.5g PVA electrolyte. Three different electrode cell internal structures were used in this experiment: a working electrode made of V2O5; a reference electrode made of saturated calomel; and a negative electrode made of platinum. The cyclic voltammetry test was carried out at a specific scan rate in a potential window spanning from -1.5 to +1.8 V. Current densities in the range of -1.5 to +1.8 V were used to characterise the charge-discharge behaviour of the material under investigation.

IV. RESULTS AND DISCUSSION

Structure analysis

On the 0^o to 90^o scale, powder X-ray diffraction was used to examine chemically formulated V_2O_5 nanoparticles. By comparing to JCPDS Card No. 00-041-1426, the *hkl* values for 2θ values were often the most precise. The peaks in the XRD pattern correlated with JCPDS show the V_2O_5 particle's systematic structure and the absence of unrelated peaks, indicating the purity of the sample. It has been determined that a few peaks with higher intensities of 2θ levels have hkl values of (200), (001), (101), (110), (112) and (301) as shown in Figure1(a). The table below shows the various types of

values discovered during the extensive analysis of this pattern. This crystal structure has a P_{mmn} space group, a D_{2h} character, and a centrosymmetric form [9]. The above data was used to analyse it from a variety of perspectives in order to assess the consistency of V_2O_5. The Debye-Scherrer formula was used to quantify and tabulate the size and dislocation density of nanocrystals with extreme precision [10].

$$D = 0.9\lambda/\beta \cos\theta \qquad (1)$$

The shape factor is 0.9, the wavelength is 0.15406 nm, the β magnitude is determined from the FWHM measure, and the value was obtained from Bragg's angle. The following relationship calculated the strain: (2) [11],

$$\boldsymbol{\varepsilon} = \beta \cos\theta / 4 \sin\theta \qquad (2)$$

This strain was determined by calculating the slope induced by β cos θ and 4 sin θ on a scale. Figure1(b) shows the Williamson-Hall plot. The strain value got from the slope. the following equation (3) shows the value of dislocation density. (Degree of Crystelanity)

$$\delta = 1/D^2 \qquad (3)$$

Table 1. Lattice parameters, crystal system, crystallite size, dislocation density and strain of V_2O_5.

SN.	Structure	Lattice parameters (Å)	Interfacial Angles (deg)	Grain size(D) nm	Dislocation density(δ) $\times 10^{14}$ m^{-2}	Micro strain (ε)	Density g/cm^3	Volume 10^6/m^3	Space group
1	Orthorhombic	a = 11.516 b = 3.5648 c = 4.379C	α = 90 β = 90 γ = 90	33.58	9.18	0.196	3.32	179.55	P_{mmn}

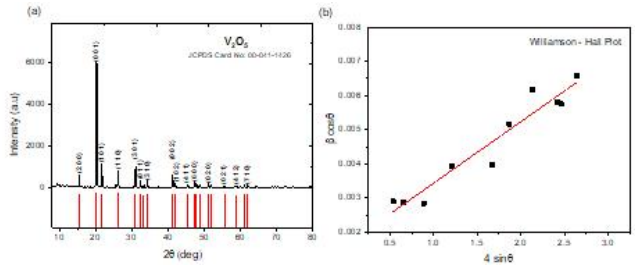

Figure1: (a)XRD spectra of a synthesised V_2O_5, and (b) Williamson hall plot for V_2O_5

UV - Vis absorption spectroscopy

The 200 to 800 nm range of the UV-Vis spectrum is used to analyse the nanomaterials. Figure2(a) shows the optical absorption spectrum of V_2O_5 nanoparticles at a wavelength. From the valence band to the conduction band of an optical transition of electrons, which exhibits the optical band gap of the material.

The absorption edge is a significant optical property for the nanomaterials. The absorption edge is a significant optical property for the nanomaterials. The edge confirms the direct or indirect optical band gap transition of the synthesised material. For optical applications, the absorption coefficient (α) is a critical parameter. The following is the formula for calculating the absorption coefficient (α) [12-13]

$$\alpha = (2.303\ A)/d \qquad (4)$$

where 'A' is the constant and 'd' denotes the thickness. In the Tauc relationship, the following formula plots the optical band gap (E_g) with respect to the absorption coefficient (α) and photon energy (hυ).

$$\alpha h\upsilon = B\ (h\upsilon - E_g)^m \qquad (5)$$

where 'B' is the constant and 'm' is the index, which depends on the mechanism of inter-band transitions, where 'm' is 2 and 1/2, corresponding to indirect and direct transitions, respectively. Figure2(b) depicts the energy connection between the direct band gap $(\alpha h\upsilon)^2$ and the indirect band gap $(\alpha h\upsilon)^{1/2}$ resulting in a direct band gap value of 4.82 eV for the V_2O_5 nanomaterials.

The most essential features of the crystal, such as refractive index (n) and extinction coefficient (k), were plotted using UV-Vis light waves, followed by a graph of the optical real dielectric constants (ε_r) and imaginary dielectric constants (ε_i) using the following formulae: This makes it possible to detect the crystal's polarisation precisely. The following equation is used to calculate k, ε_r and ε_i [14-15].

$$k = \lambda\alpha/4\pi \qquad (6)$$

$$\varepsilon_r = n^2 - k^2 \qquad (7)$$

$$\varepsilon_i = 2nk \qquad (8)$$

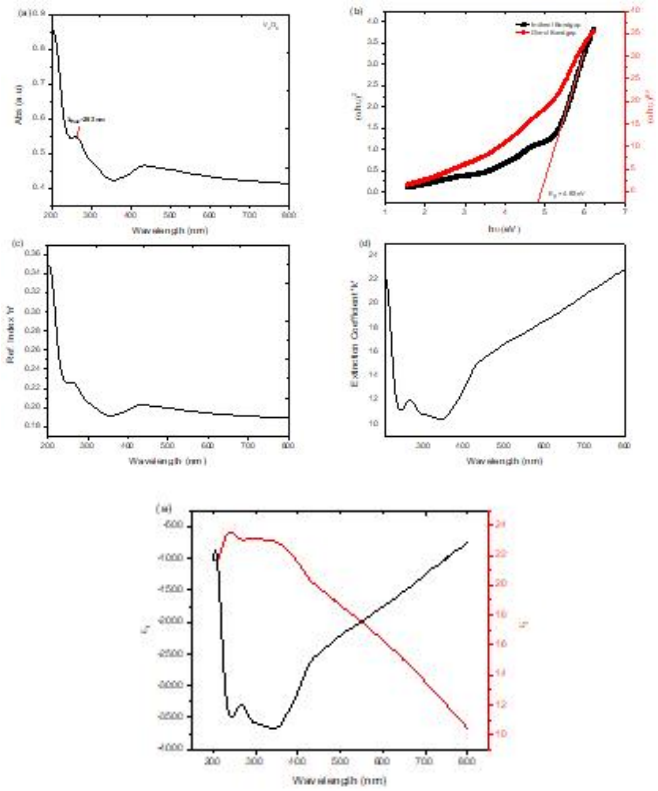

Figure2. (a) Wavelength with V_2O_5 nanoparticles based on optical absorption, (b) Direct and indirect band gap for the material, (c) Refractive index number '*n*', (d) extinction coefficient '*k*' and (e) the real ε_r and imaginary ε_i parts of the dielectric constant for the material.

Photoluminescence Spectroscopy

Data collected under this spectroscopic method provides high sensitivity and quality information regarding the presence of a specific structure, emission band, defect, and defect state up to a single molecular level. The maximum emission peak recorded at 655 nm and the corresponding band value have been 1.89 eV. According to the recombination of electron-hole pairs, the intense emission peak shows at 655 nm [16]. Identified the red colour in emissions for V_2O_5 nanomaterials, which leads us to conclude that the peak arises from the lowest split-off V 3d band to the O 2p valence band [17-18].

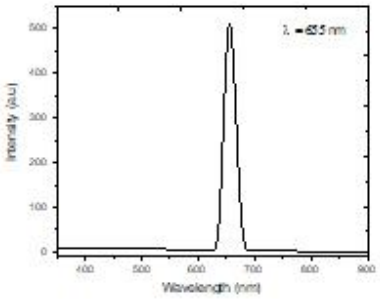

Figure 3. PL emission spectra of V_2O_5 nanoparticles and the sample was excited at 655 nm.

Vibrational spectroscopy

Fig. 4 shows the material's FTIR analysis, which is done on a KBr medium with a wave number ranging from 400 to 4000 cm^{-1}. With the V_2O_5 system, the peak with a wave number of 463 cm-1 indicates the stretching of V = O [19], while the peaks with wave numbers of 517 and 836 cm^{-1} correspond to the symmetrical and asymmetric stretching, respectively, of the V-O-V system [20–21]. The strongest ion bond with bending vibration is shown by the maximum peak at 1383 cm^{-1}[22]. The 3400cm^{-1} band represents O-H stretching mode. The force constant value of the material has been calculated as 3.07 N/cm.

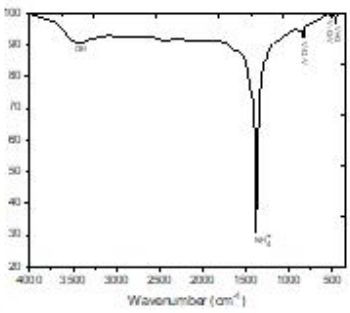

Figure 4.FTIR spectra of V_2O_5 nanoparticles.

SEM analysis

Fig. 5, showing the images of V_2O_5 nanoparticles at two different magnifications, were made in a time-efficient autoclave and analysed using the scanning electron microscope (SEM). This process of synthesisation produces particles with a fine structure of nanoparticle size that are strewn across a large region, as shown in the images It is clear from this inference that the calcination approach, in conjunction with the hydrothermal process, has prepared the way for the production of nanoparticles of high quality. A uniform distribution with acceptable particle sizes further enriches the subject of electrochemical research and analysis.

The histogram image shows the average particle distribution, that also conform the particles are present in nanosize.

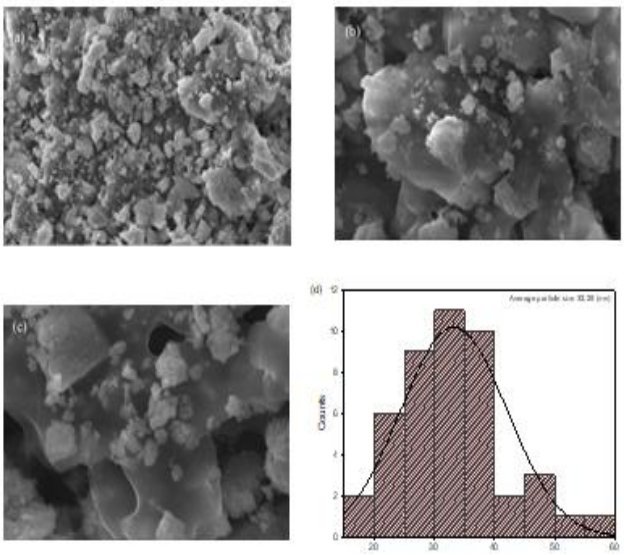

Figure 5.(a), (b) and (c) SEM images showing the morphology of V_2O_5nanomaterials, (d) The histogram of particle size distribution derived from the SEM images.

Cyclic Voltammetry

For the electrochemical behaviour of V_2O_5 nanoparticles, a cyclic voltmeter and galvanostatic charge discharge technique were utilised to measure voltage and current. The scan reveals the CV traces of the V_2O_5 particles and the specific capacitance computed from the CV curves using the following formula: [23]

$$C = \frac{Q}{m\Delta V} \qquad (9)$$

Where '*C*' refers to the specific capacitance of the material, '*Q*' refers to the average charge duration of anodic and cathodic, '*m*' refers to the mass of the active material, and '*V*' denotes the potential window. The specific capacitance of the V_2O_5 electrode was determined to be 521 Fg^{-1} at a scan rate of 2 mVs^{-1}, which corresponded to the greatest possible scan rate of synthesised material.

Fig. 6(b) depicts the charge-discharge patterns of V_2O_5 samples when subjected to a certain current level. It is possible to compute the specific capacitance (*C*), energy density (*E*) and power density (*P*) of the electrodes by using the following equations: [7-8]

$$C = \frac{i\Delta t}{m\Delta V} \qquad (10)$$

$$E = \frac{1}{2} C\,(\Delta V)^2 \qquad (11)$$

$$P = \frac{E}{\Delta t} \qquad (12)$$

where '*i*' represents the specific current, '*t*' represents the discharge time, '*m*' represents the mass of the active material, '*V*' represents the potential window, '*E*' represents the energy density ($Whkg^{-1}$) and '*P*' represents the power density ($kWkg^{-1}$). The specific capacitance of the V_2O_5 sample reached a maximum of 444 Fg^{-1} when subjected to a current density of 1 Ag^{-1} at room temperature.

According to (11) and (12) equations, the estimated *E* at a current density of 1 Ag^{-1} of V_2O_5 is 128 $Whkg^{-1}$ and the associated *P* is 1.33 $kWkg^{-1}$, demonstrating the superior electrochemical performance of V_2O_5 nanoparticles. The nanostructured V_2O_5 produced by the accepted chemical procedure has the expected capability.

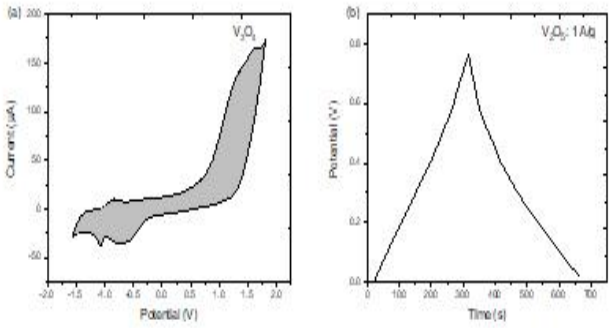

Figure6. (a) CV curves of V_2O_5 nanomaterial, (b) Potential vs. time for charge and discharge profile of a current density of 1A g^{-1}

V. CONCLUSION

The time-efficient microwave autoclave technique developed the V_2O_5 nanoparticles. The reaction time has a significant influence on determining the morphology, so this technique gives a shaped nanoparticle. It has proven the nanomaterial to have structural and optical properties by using several techniques, such as XRD, UV-Vis, PL, FTIR, and CV analysis. The crystalline nature was confirmed by XRD, and its average particle size and dislocation density were estimated at 33 nm and 9.18×10^{14} m^{-2}, respectively. As coded in the JCPDS-00-041-1426 file, it has an orthorhombic crystal structure with a prominent (001) orientation. Based on the Williamson Hall plot, it was estimated that the microstrain was 0.196. These data show that the UV-Vis absorption spectrum at 263 nm has the maximum absorption value, and the Tauc plot was used to identify the direct band gap. The graphs of the refractive index, extinction coefficient, and real-

imaginary dielectric constants were explained. According to the PL spectral region, the emission intensity is 655 nm, indicating that the synthesised V_2O_5 easily emits red radiation and is thus well-suited for the production of LEDs. The presence of different functional groups in the material was verified by measuring the vibration of the molecules using FTIR spectroscopy. The average size of the V2O5 particle, determined by XRD and SEM smooth surface morphology, proves the material is nanometers in size. High specific capacitance, energy density, and power density were seen in the electrochemical characteristics of synthesised V_2O_5 used as an working electrode.

All the main points of the research work are written in this section. Ensure that abstract and conclusion should not same. Graph and tables should not use in conclusion.

REFERENCES

[1] FrançoisBéguin and Elżbieta Frąckowiak, " Super capacitors: Materials, Systems, and Applications", Wiley- VCH Verlag GmbH & Co. KGaA, Vol 1, [2013].

[2] Galizzoli D, Tantardini F, Trasatti S," Ruthenium dioxide: a new electrode material. II. Non-stoichiometry and energetics of electrode reactions in acid solutions" , Journal of Applied Electrochemistry, Vol 5, 203-214, [1975].

[3] A. MottramCouper, Derek Pletcher and Frank C. Walsh, " Electrode materials for electrosynthesis", Chemical Reviews, Vol 90, 837-865, [1990].

[4] Chi-Chang Hu and Wei-Chun Chen, " Effects of substrates on the capacitive performance of $RuO_x \cdot nH_2O$ and activated carbon–RuO_x electrodes for supercapacitors" ,ElectrochimicaActa, Vol 49, 3469-3477, [2004].

[5] Satoshi Horikoshi and Nick Serpone, "Microwaves in Nanoparticle Synthesis: Fundamentals and Applications", Wiley- VCH Verlag GmbH & Co. KGaA, Vol 1, [2013]

[6] Chao Zhong, Jiazhao Wang, Zhixin Chen and Huakun Liu, " SnO_2–Graphene Composite Synthesized via an Ultrafast and Environmentally Friendly Microwave Autoclave Method and Its Use as a Superior Anode for Lithium-Ion Batteries", The Journal of Physical Chemistry C, Vol 115, 25115-25120, [2011].

[7] M. Dhananjaya, N. Guru Prakash, G. Lakshmi Sandhya, A. Lakshmi Narayana and O.M. Hussain,"Microstructure and Supercapacitor Properties of V_2O_5 Thin Film Prepared by Thermal Evaporation Method", Mech Materials Science & Engineering, DOI: 10.2412/mmse.88.66.781, [2017].

[8] S. Nandhini, N. Maheswari and G. Muralidharan,"Electrochemical behavior of novel β−Mn_3O_4/V_2O_5 electrode using gel electrolyte for high performance supercapacitors", AIP,DOI: 10.1063/1.4980273, [2017].

[9] Jenny P. Glusker, Mitchell Lewis and Miriam Rossi," Crystal Structure Analysis for Chemists and Biologists", Wiley-VCH, ISBN: 978-0-471-18543-7, [1994].

[10] Majidfarahmandjou and NilofarAbaeiyan, "Chemical Synthesis of Vanadium Oxide (V_2O_5) Nanoparticles Prepared by Sodium Metavanadate", Journal of Nanomedicine Research, Vol 5, [2017].

[11] DebojyotiNath, Fouran Singh and Ratan Das, "X-ray diffraction analysis by Williamson-Hall, Halder-Wagner and size-strain plot methods of CdSe nanoparticles- a comparative study", Materials Chemistry and Physics, Vol 239, 122021,[2020].

[12] Imen Ben Saad, NajehHannachi, Thierry Roisnely and FaouziHlel, "Optical, UV-Vis spectroscopy studies, electrical and dielectric properties of transition metal-based of the novel organic–inorganic hybrid $(C_6H_{10}N_2)(Hg_2Cl_5)_2.3H_2O$", Journal of Advanced Dielectrics, Vol 9, 1950040,[2019].

[13] Wasi Khan, Z. A. Khan, A. A. Saad, S. Shervani, A. Saleem and A. H. Naqvi, "Synthesis and characterization of Al doped ZnO nanoparticles", International Journal of Modern Physics: Conference Series, Vol 22, 630-636, [2013].

[14] Suresh Sagadevan and JibanPodder, "Optical and Electrical Properties of Nanocrystalline SnO_2 Thin Films Synthesized by Chemical Bath Deposition Method", Soft Nanoscience Letters, Vol 5, 55-64,[2015].

[15] WiktorMatysiak, Tomasz Tański and WeronikaSmok, " Study of optical and dielectric constants of hybrid SnO2 electrospun nanostructures", Applied Physics A, Vol 126, [2020].

[16] Stefano Sanguinetti, Mario Guzzi and Massimo Gurioli, "Accessing structural and electronic properties of semiconductor nanostructures via photoluminescence", Characterization of Semiconductor Heterostructures and Nanostructures, 175-208, [2008].

[17] C. Diaz, G. Barrera, M. Segovia, M. L. Valenzuela, M. Osiak and C. O'Dwyer, " Crystallizing Vanadium Pentoxide Nanostructures in the Solid-State Using Modified Block Copolymer and Chitosan Complexes", Journal of Nanomaterials, Vol 2015, 1-13, [2015].

[18] Nilima V. Hullavarad, Shiva S. Hullavarad and Pramod C. Karulkar, " Electrical and Optical Properties of V_2O_5 Micro-Nano Structures Grown by Direct Vapor Phase Deposition Method", Journal of The Electrochemical Society, Vol 155, K84, [2008].

[19] Yingjie Wu, GuohuaGao and Guangming Wu, "Self-assembled three-dimensional hierarchical porous V_2O_5/graphene hybrid aerogels for supercapacitors with

high energy density and long cycle life", Journal of Materials Chemistry A, Vol 3, 1828-1832, [2015].

[20] Cheng Zhang, Guozhao Fang, Caiwu Liang, Jiang Zhou, Xiaoping Tan, Anqiang Pan and Shuquan Liang, "Template-free synthesis of highly porous V_2O_5 cuboids with enhanced performance for lithium ion batteries", Nanotechnology, Vol 27, 305404,[2016].

[21] P. Ragupathy, S. Shivakumara, H. N. Vasan and N. Munichandraiah, "Preparation of Nanostrip V_2O_5 by the Polyol Method and Its Electrochemical Characterization as Cathode Material for Rechargeable Lithium Batteries", The Journal of Physical Chemistry C, Vol 112, 16700-16707, [2008].

[22] Mathieu Gautier, Fabrice Muller, Lydie Le Forestier, Jean-Michel Bény and RégisGuégan, "NH_4-smectite: Characterization, hydration properties and hydro mechanical behaviour", Applied Clay Science, Vol 49, 247-254, [2010].

[23] Yifu Zhang and Yuting Huang, "Facile synthesis and characterization of rough surface V_2O_5nanomaterials for pseudo-supercapacitor electrode material with high capacitance", Bulletin of Materials Science, Vol 40, 1137-1149, [2017].